Bio-based Molecular Imprinted Polymers for Separation and Purification of Chlorogenic Acid Extracted from Food Waste

Yagya Gupta,^{1,2} Laura Elizabeth Beckett,³ Sunitha Sadula,² Vibin Vargheese,^{1,2} LaShanda Korley,^{1,3}Dionisios G. Vlachos^{1,2*}

¹Department of Chemical & Biomolecular Engineering, University of Delaware, 150

Academy St., Newark, DE 19716, USA.

²Catalysis Center for Energy Innovation, RAPID Manufacturing Institute, and Delaware Energy Institute (DEI), University of Delaware, 221 Academy St., Newark, DE 19716, USA.

³Center for Research in Soft Matter and Polymers, and Department of Materials Science and Engineering, University of Delaware, 150 Academy St., Newark, DE 19716, USA.

Keywords: molecular imprinted polymers, HSPiP, COSMO-RS, antioxidants, chlorogenic acid, food waste

Abstract

Food waste is a profound challenge as 17% of global food production (i.e., 931 million tons) ends up as waste yearly. A cost-effective strategy is the extraction of high-value phenolic

acids from food waste, but their downstream purification is challenging owing to their similar chemical nature, high boiling points, and low concentrations in complex mixtures. Herein, we propose separating target phenolics using molecular imprinted polymers. The stability of the monomer-template complex during the synthesis is critical in optimizing the polymer selectivity and performance. COnductor like Screening MOdel for Real Solvents (COSMO-RS) and Hansen Solubility Parameters in Practice (HSPiP) computations were used to screen the interaction of 28 monomers and 13 porogenic solvents with chlorogenic acid as the target molecule. Experiments revealed that itaconic acid, the functional monomer, and THF, the synthesis solvent, provide the highest reported separation factor. The polymer exhibits superior selectivity towards chlorogenic acid in concentrated solutions of up to 1 mg/mL, and its high sensitivity to various functionalities enables the effective separation of all target phenolic acids. The polymer's performance was evaluated in different extraction solvents, and Fourier transform infrared (FTIR) studies revealed polymer-solvent interaction as the critical factor influencing its performance. The application of the polymer in purifying up to 92% chlorogenic acid from coffee beans and potato peel waste extractives is demonstrated, and its reusability is evaluated. In contrast to the current industrial purification methodology that produces mixtures, the proposed technology provides at least eleven times higher economic value and 95% less carbon emissions based on lab-scale techno-economic analysis.

Introduction

Food waste (FW) is a global challenge with ~17% of global food production, estimated to be 931 million tons annually, ending as waste.[1] Current FW management, such as anaerobic digestion,[2] composting,[3] fermentation,[4] and animal feed, produce low-value products, i.e., biogas, compost, and ethanol. Alternative valorization strategies are required to reduce greenhouse gas emissions[5] and the long processing times of current technologies.

The extraction of phenolic acids as natural antioxidants is a lucrative alternative. Synthetic antioxidants, such as butylated hydroxyanisole, butylated hydroxytoluene, propyl gallate, and tert-butyl hydroquinone, are toxic.[6–8] Natural antioxidants, such as chlorogenic, caffeic, *p*-coumaric, and ferulic acids, are encouraged in the pharmaceutical, food, and cosmetic industries.[9] The chlorogenic acid market includes *p*-coumaric and caffeic acid, collectively valued at \$132.2 million USD, while the market size for ferulic acid is \$68 million USD.[10,11] These phenolics can also be converted to BTX (benzene, toluene, and xylene) currently produced from petroleum, but these are lower-value products.

Various mixtures of antioxidant powders extracted from plants and biomass are currently industrially produced. Nutragreen,[12] Euromed,[13] Cymbio Pharma,[14] Flavor Trove,[15] and Applied Food Sciences,[16] produce coffee bean extracts containing caffeine, chlorogenic, and other hydroxycinnamic acids (see Supplementary Table 1 for product description). Kao Corporation reported a method to extract and purify 90% chlorogenic acid from raw or roasted coffee beans (see Supplementary Figure 1).[17] The product is a mixture of nine monocaffeoylquinic, ferulaquinic, and dicaffeoylquinic acids. The antioxidant capacity of mixtures depends on the compounds' molecular structures, intermolecular interactions, and concentrations.[18–20] For instance, a mixture of acids extracted from green coffee beans has a lower antioxidant capacity than pure chlorogenic acid.[21] Thus, purifying target phenolic acids as replacements for synthetic antioxidants is desirable.

The purification of phenolic acids post-extraction is challenging because of their structural similarity, high and similar boiling points, and similar chemical functionality. As a result, traditional separation methods, such as distillation, membrane separation, and ionic resin adsorption, are inept. Molecular imprinted polymers conduct structural recognition-based separations. [22] The target molecule (template) is imprinted on the polymer and then washed with a solvent to leave behind a cavity (Figure 1). Due to their molecular match and interactions, such as hydrogen bonds, van der Waals forces, and electrostatic interactions, these cavities selectively adsorb the target molecule from a mixture. The polymer is washed with a solvent to extract the target compound and regenerate the adsorption sites. The solvent can then be evaporated to collect a purified compound. The high selectivity of these polymers

enables their diverse applications in chromatography,[23,24] purification,[25] sensing,[26] detection,[27,28] catalysis,[29] and drug delivery.[30,31] Previously, molecular imprinted polymers have been employed for chlorogenic acid purification.[32,33] Li et al. developed an imprinted polymer monolithic stationary phase for purifying chlorogenic acid extracted from *E. ulmodies* leaves by selectively adsorbing the other compounds. [34] The approach provides low-purity chlorogenic acid, as the adsorbent does not preferentially take up all co-existing compounds. Hao et al.[35] and Zhao et al.[36] conducted column chromatography with imprinted polymers to extract chlorogenic acid from spiked fruit juices and honeysuckle samples. These chromatographic methods offer a narrow range of operation and scale-up challenges, rendering them useful for analytical purposes. To our knowledge, the implementation of a bio-based molecular imprinted polymer for separating target phenolic acids post-extraction from FW has not been reported.

Here, we synthesize molecular imprinted polymer to selectively separate commercially valuable phenolic acids from a FW-extracted mixture. We introduce the Hansen Solubility Parameters in Practice (HSPiP) model to identify monomers and solvents based on their molecular interaction with the target compounds for imprinted polymer synthesis. We employ the COnductor like Screening MOdel for Real Solvents (COSMO-RS) multiscale simulation generated sigma profiles to understand the molecular behavior of different monomers and their performance as a molecular imprinted polymer. We conduct experiments to identify the best monomer and solvent for polymer synthesis, characterize the resulting polymers, and evaluate their performance in different phenolic mixtures,

extraction solvents, and a broad concentration range. Fourier transform infrared (FTIR) analysis confirms the structure of polymers and their interaction with the solvents. The separation strategy is demonstrated on potato peel and spent coffee bean waste. Lab-scale technoeconomic analysis reveals the economic and environmental advantages of the proposed technology over commercial alternatives, distinguishing it from existing studies focused solely on analytical applications of imprinted polymers.

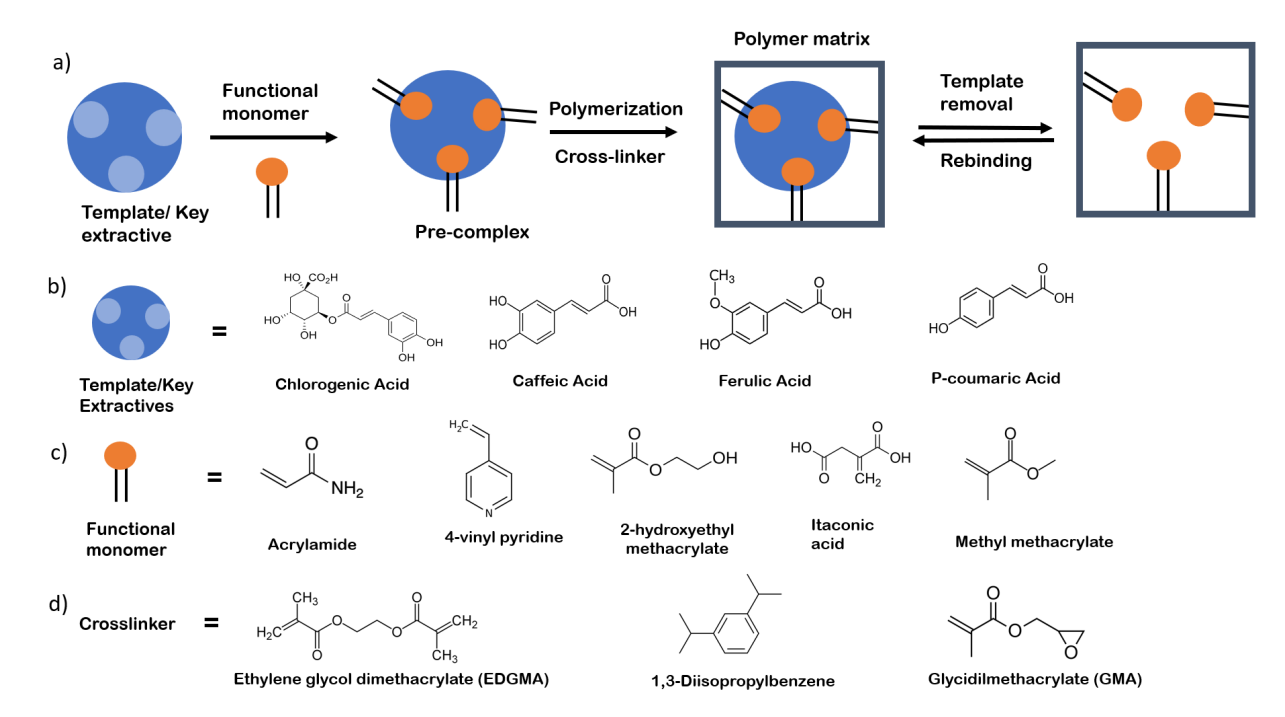


Figure 1: Molecular imprinted polymer synthesis. a) Strategy and adsorption mechanism for molecular imprinted polymers demonstrating chemical structures of b) template, c) functional monomer, and d) crosslinker.

Materials and Methods

Materials

Acrylamide (GC grade (purity \geq 98%)), itaconic acid (purity \geq 99%), 2,6-diaminopyridine (GC grade (purity \geq 97%), o-aminophenol (purity \geq 99%), ethylene glycol dimethacrylate (EDGMA) (purity \geq 98%), 2,2-azobisisobutyronitrile and caffeic acid (HPLC grade (purity \geq 98%)) were purchased from Sigma Aldrich. *p*-Coumaric acid (purity 98%), chlorogenic acid (purity 99.45%), ferulic acid (purity 99.4%), 2-hydroxyethyl methacrylate (purity \geq 97%), and o-phenylenediamine (purity \geq 98%) were purchased from Fisher Scientific. ASTM-Type 1 grade deionized (DI) water (Milli-Q ® Direct) was used in all experiments. Solvents N,N-dimethylformamide (HPLC grade, purity \geq 99.9%), methanol (ACS reagent, purity \geq 99.5%), and ethanol (ACS reagent, purity \geq 99.5%) were obtained from Sigma Aldrich. Tetrahydrofuran (HPLC grade, purity \geq 99.5%) was obtained from Fisher Scientific.

Synthesis of molecularly imprinted polymers and non-imprinted polymers

The template molecule and a functional monomer at a ratio of 1:4 were added to 5 mL of tetrahydrofuran (THF). The mixture was stirred at room temperature in N2 for 30 min. 0.03 g of 2,2-azobisisobutyronitrile recrystallized with methanol and crosslinker EDGMA were added to the mixture such that the monomer and crosslinker weight by volume was 53.3%. The monomer-to-crosslinker ratio was 1:3. The solution was purged under nitrogen for 15 min and sealed. The polymerization proceeded for 24 h at 75 °C. The resulting polymer was ultrasonicated in methanol for 1 h to remove the template and dried under vacuum at 50 °C. The template extraction efficiency was determined to be 96% using HPLC. The polymer was

grounded using a Thomas Wiley® Mini Cutting Mills to a powder of size < 0.5 mm. A non-imprinted polymer was synthesized with the same methodology without a template and ultrasonication.

Adsorbent characterization

The porosity of the synthesized polymers was determined by nitrogen gas sorption at –196 °C using the Micromeritics ASAP 2020 Brunauer Emmett Teller (BET) Analyzer. TGA was performed using a TA instruments Q600 SDT thermogravimetric analyzer and differential scanning calorimeter (DSC) for a temperature program of 30 to 700 °C at a heating rate of 10 K min⁻¹ under air (30 mL min⁻¹). Scanning electron microscopy (SEM) was conducted using an AURIGA 60 Crossbeam FIB-SEM with an acceleration voltage of 3 kV. The specimens were coated with a thin (~5 nm) conductive layer of Pd/Au to minimize sample charging using a vacuum sputter coater (Denton Desk IV, Denton Vacuum, LLC). A Specac Golden Gate diamond attenuated total reflectance (ATR) unit gave the FTIR spectra, with a 4 cm⁻¹ resolution in the 4000-1000 cm⁻¹ range using a Thermo Scientific Nicolet iS50 spectrometer instrument equipped with an MCT-B detector. Solutions (1 to 0.125 mg/µl) of chlorogenic acid and a saturated polymer mixture in a solvent (DMF, water, or ethanol) were analyzed.

The swelling ratio of the polymer was measured in DMF, water, and ethanol. 100 mg of dry polymer was weighed in a tube, and 1-1.5 mL of solvent was added. The tube was sealed,

stirred for 2 h at 25°C, and centrifuged. The supernatant was drained, and the excess solvent was wiped off. The wet polymer was weighed, and the swelling ratio was estimated (Eq. 1).

$$Swelling \ ratio = \frac{Weight \ of \ wet \ polymer-weight \ of \ dry \ polymer}{Weight \ of \ dry \ polymer} \tag{1}$$

Quantification of phenolic compounds

The standard acids concentration was quantified using high-performance liquid chromatography (HPLC) using a Waters e2695 separations module coupled to a Waters 2414 refractive index meter and a Waters 2998 photodiode array detector. An Agilent Zorbax SB-C18, 250 mm column was used at 323 K, using solvent A (pure methanol) and solvent B (1% formic acid in water) as a mobile phase flowing at 0.8 mL/min. A gradient method was set up for 0% B to reach 95% B in 5 min. The concentration was calculated from the absorbance peak area measured between 320 to 380 nm at the respective retention time based on pure compound calibrations.

The FW-extracted acids were identified, and their concentration was quantified using Ultra performance liquid chromatography-mass spectrometry (UPLC-MS) on a Q-orbitrap mass spectrometer. A Waters Acquity UPLC BEH C18 column (1.7 µm 2.1 X 30 mm) was used with solvent A (water containing 0.1% formic acid) and solvent B (acetonitrile containing 0.1% formic acid) as the mobile phase flowing at 0.5 mL/min. A gradient method was set up for 0% B to reach 95% B in 5 min.

Single and multi-component adsorption

For single component adsorption, a stock solution of chlorogenic acid in a solvent at 0.4, 5, 8, 10, 20, 50, and 100 mg/mL was made. For multicomponent adsorption, a stock solution of an equal concentration (in the range 0.1–30 mg/mL) mixture of chlorogenic, *p*-coumaric, caffeic, and ferulic acids was made in DMF, water, and ethanol. 2 mg of polymer was added to a vial containing 2 mL of stock solution. The mixture was stirred for 2 h at 298 K. All experiments were conducted in triplicates. 0.45 µm syringe filters were used for sampling. HPLC was used for quantification.

Extraction from FW

In our recent study, we established that DMF is an excellent solvent for extracting target phenolics owing to its superior polarity and hydrogen bond-accepting character.[37] Thus, 20 mL of DMF and 1 g of FW feedstock (spent coffee bean or potato peel waste) were added to a round bottom flask. The target compounds are thermally degradable.[38–40] Thus, the mixture was stirred and heated to 60°C for 2 h (short times and lower temperatures). The solution was then filtered and quantified on UPLC-MS.

Adsorption from FW Extract

10~mg of adsorbent was added to 10~mL of FW extracted solution. The mixture was stirred for 2~h at 298~K. Duplicate experiments were conducted. $0.45~\mu m$ syringe filters were used for sampling. The samples were quantified using UPLC-MS.

Computations

We employed the HSPiP (HSPiP 5.3.05) for the selection of monomers and solvents for polymer synthesis. The HSPiP distance (Ra) between two compounds provides their 'likeness': Ra² = $4(\delta D_1 - \delta D_2)^2 + (\delta P_1 - \delta P_2)^2 + (\delta H_1 - \delta H_2)^2$ where δD , δP , and δH is dispersion, polar and hydrogen bonding energy. The uncertainty associated with the experimentally determined HSP and predicted distance are \pm 0.5 (MPA)^{0.5} and \pm 1 (MPA)^{0.5}, respectively.[41] Given its approximations, we employed the ADF COSMO-RS implementation in the ADF2020.101 modeling suite to generate monomers' σ-profiles to understand their molecular behavior. The molecules are optimized in a vacuum using density functional theory (DFT) for sigma profile generation. For geometry optimization, we used the TZP small-core basis set, the Becke-Perdew (GGA: BP86) functional, the scalar ZORA, and the numerical integration quality of 4 with an energy convergence criteria 10-5 Ha. The approximations of COSMO-RS in the acid dissociation factor, long-range interactions, weak intermolecular forces, and molecule conformations affect its accuracy.[41,42] Despite these limitations, the computational tools can rapidly screen molecular databases to guide

experimental efforts. Experiments are, however, necessary for validating and identifying the best system.

Results and Discussion

In the following sections, we discuss the computations-aided polymer design, its experimental assessment, and insights into the optimized polymer's morphological, molecular, and thermal properties. We analyze the selectivity of the polymer in a mixture of target acids and its concentration range of effective separation. We then determine its versatility as an adsorbent by evaluating its stability and performance in common extraction solvents. We assess the polymer's suitability for large-scale applications by examining its reusability and efficacy in selectively purifying chlorogenic acid (model target acid) from two FW feedstocks. Finally, we evaluate the economic and environmental advantages of the proposed method and contrast it with existing commercial technology.

Polymer design

Stable pre-polymerization complexes are crucial in non-covalent imprinting technology to obtain selective recognition sites.[43–46] The monomer, template, and solvent interactions dictate the stability of such complexes.

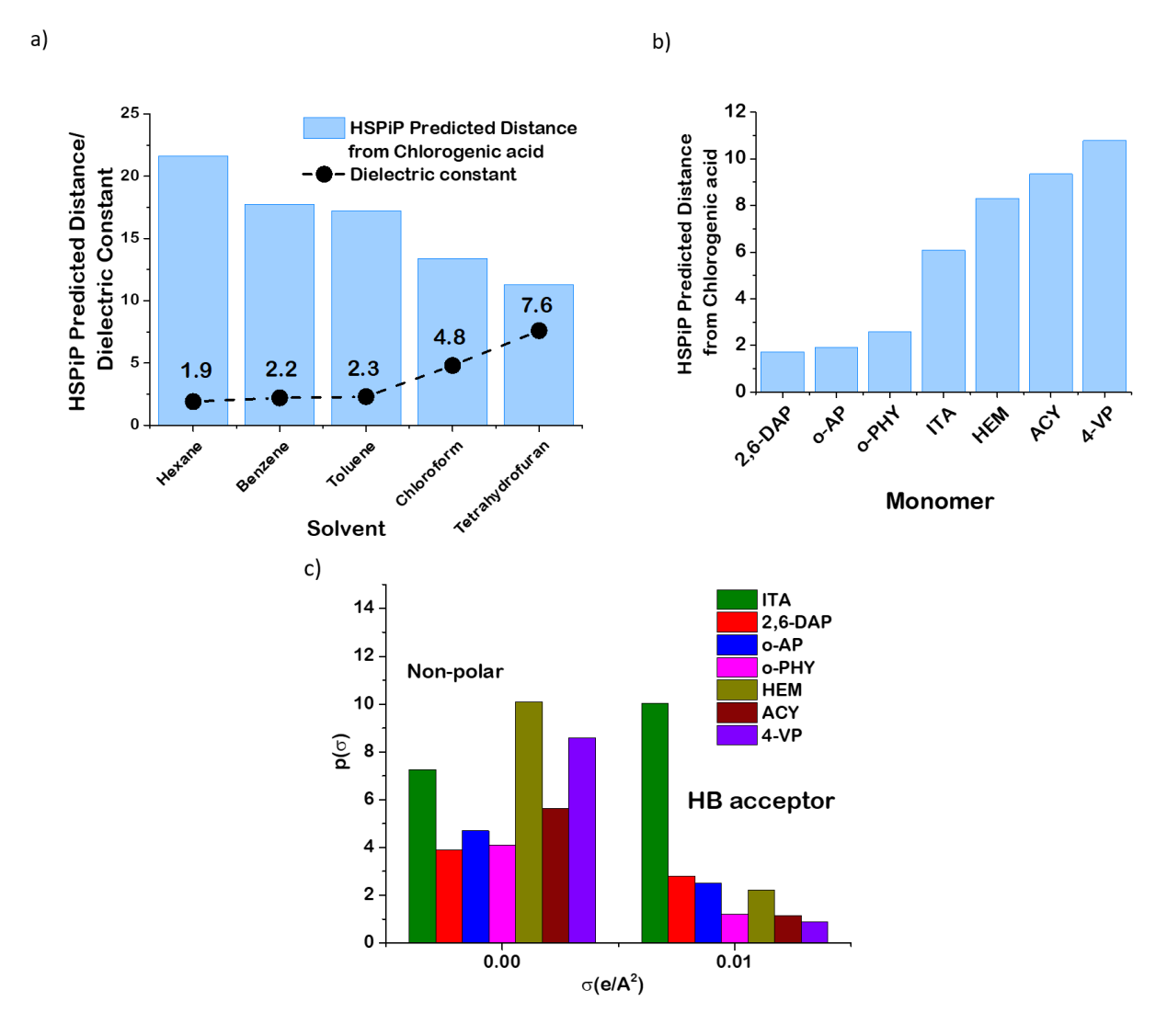


Figure 2: Model-guided solvent and monomer selection for polymer synthesis. a) Dielectric constant of various solvents and their HSPiP predicted distance from chlorogenic acid. [47–49] The dashed line is drawn for visual guidance. b) HSPiP-predicted distance of various monomers from chlorogenic acid. c) COSMO-RS computed surface charge density of different monomers at $\sigma(e/Å^2) = 0$ and 0.01. 2,6-DAP, σ -AP, σ -PHY, ITA, HEM, ACY, and 4-VP stand for 2,6-diaminopyridine, σ -aminophenol, σ -phenylenediamine, itaconic acid, 2-hydroxyethyl methacrylate, acrylamide, and 4-vinyl pyridine, respectively.

HSPiP and COSMO-RS Predictions

For solvent selection, we use dielectric constants compiled from the literature as a measure of their polarity.[50,51] Since the template is polar (see Supplementary Table 2 for target compounds' HSP), polar solvents would hinder its interactions with the monomer. In contrast, a non-polar solvent would enhance the stability of the pre-polymerization complex.[52-54] Thus, we selected 5 of 13 recommended porogenic solvents (see their dielectric constants and HSP in Supplementary Table 3) with the lowest dielectric constants (Figure 2a).[47-49] As the solvent brings monomer and template in one phase, their solubility in the solvent is also important. We applied HSPiP (Figure 2a) and COSMO-RS (see Supplementary Table 4 for solubility estimates) to estimate the likeability and solubility of chlorogenic acid (model template) and target monomers in the selected solvents. Nonpolar solvents like hexane, benzene, toluene, and chloroform provide very low solubility for the monomers and chlorogenic acid, making polymer synthesis non-viable. THF provides good solubility and has a sufficiently low dielectric constant to stabilize the complex. Consequently, THF was selected for imprinted polymer synthesis.

Acrylamide[52,55–57] and 4-vinylpyridine[43,44,58–60] are standard functional monomers for synthesizing polymers imprinted with polar bioactive compounds. For selection, we compiled a list of 28 monomers previously used for synthesizing imprinted polymers and applied HSPiP to identify the ones interacting strongly with chlorogenic acid (see Supplementary Table 5 for a comprehensive list and their HSP).[22,49,61–64] We found

acrylamide superior to 4-vinyl pyridine and 7 monomers superior to acrylamide with amines being predominant (4 out of 7). We down-selected the top 5 monomers (Figure 2b) to provide insights into monomer selection and conduct experiments. Monomers of high polarity (δP) and HB character (δH) interact strongly with the template, given its polar and HB donor nature. HSPiP indicates that amines have the highest dispersion parameter (δD). However, itaconic acid has a higher δH , and acrylamide has a higher δP . The HSP weighs its dispersion component more compared to δP and δH . As a result, the trend is 2,6diaminopyridine > 2-aminophenol > o-phenylenediamine > itaconic acid > 2-hydroxyethyl methacrylate > acrylamide > 4-vinylpyridine. The σ -profiles (Figure 2c) reveal that the amines, except 4-vinyl pyridine, have lower non-polar (at $\sigma(e/Å^2) = 0$) surface charge density $(\rho(\sigma))$ and overlapping profiles, indicating higher polarity and similar performance consistent with the HSPiP predictions (see Supplementary Figure 2 for monomers' σ-profiles). Itaconic acid has the highest HB acceptor charge density (at $\sigma(e/Å^2) > 0.0079$), connoting stronger interactions than amines in contrast to HSPiP. Finally, 2-hydroxyethyl methacrylate and 4vinyl pyridine have low polarity and HB acceptor character and interact weakly than acrylamide. Consequently, we anticipate itaconic acid to exhibit superior performance than the amines.

Experimental verification of model predictions

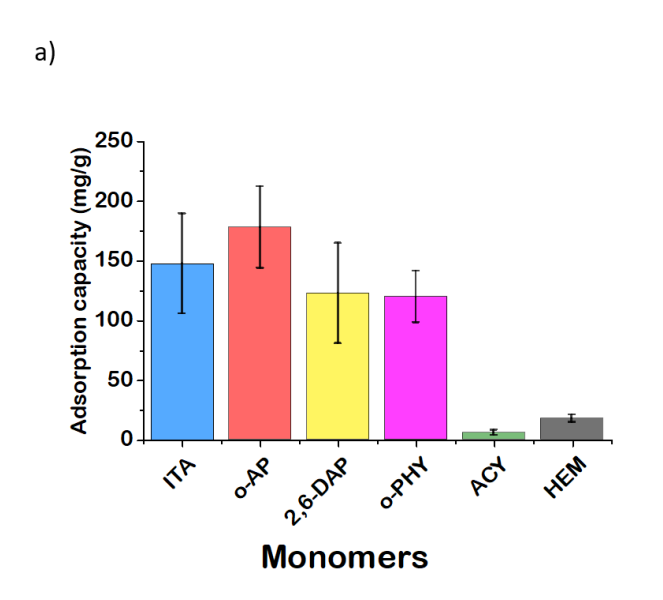
Experimentally, the polymers synthesized with the selected 5 monomers provide higher single-component adsorption capacity than the polymer with acrylamide as the functional monomer (Figure 3a). 2-hydroxyethyl methacrylate provides the lowest adsorption capacity ($^{\sim}$ 3 times that of acrylamide). The rest offer at least 20 times higher adsorption capacity than the literature standard. The adsorption capacity of the polymers made of the top four monomers is comparable, with minor variations in single-component adsorption, and are ranked as 2-aminophenol > itaconic acid > 2,6-diaminopyridine \approx o-phenylenediamine.

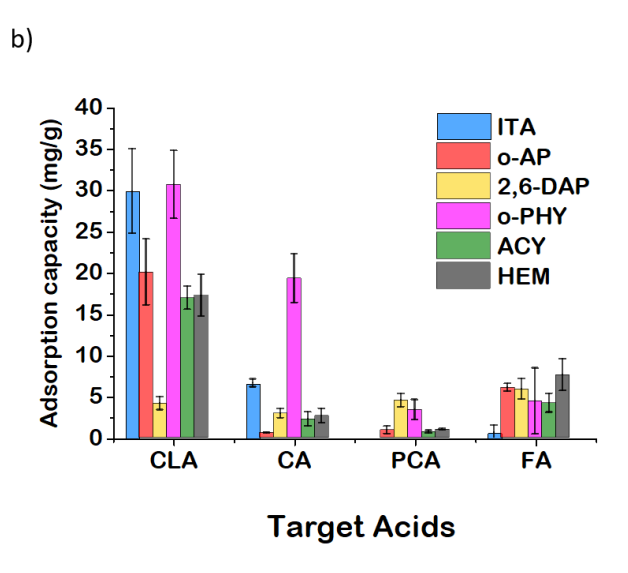
In contrast to single component data, the multicomponent adsorption (Figure 3b) reveals itaconic acid's superior performance, followed by 2-aminophenol \approx acrylamide > 2-hydroxyethyl methacrylate > o-phenylediamine > 2,6-diaminopyridine (see Supplementary Table 6 for their separation factors). Only itaconic acid provides a higher separation factor (\sim 2 times) (Eq. 2) for the template (chlorogenic acid) than acrylamide. As discussed above, the synthesized amine polymers are porous (see their BET surface area in Supplementary Table 7) but lack molecular selectivity, potentially due to lower HB character and overestimation by HSPiP. Thus, we selected itaconic acid as a suitable monomer for efficient separation.

$$Separation \ factor = \frac{\textit{Adsorption capacity of target molecule}}{\textit{Sum of adsorption capacity of all other compounds in the mixture}} \tag{2}$$

Next, we evaluate all target compounds as prospective templates. Four polymers (P1, P2, P3, and P4) were synthesized (see Supplementary Table 8 for polymer description and their

separation factors) with caffeic, chlorogenic, *p*-coumaric, and ferulic acid as the template, respectively (Figure 3c). Ideally, imprinted polymers should demonstrate the highest selectivity toward the corresponding template. However, experiments show that all polymers prefer chlorogenic acid and reject *p*-coumaric acid regardless of the template. We believe that the molecular interaction of the polymer (adsorbent) with the structurally analogous compounds (adsorbate) in a mixture leads to the observed performance.[65] Specifically, HB is a characteristic parameter of the adsorbate-adsorbent interaction.[66,67] The molecular structure of the target compounds (Figure 1) shows that chlorogenic acid has the highest number of HB sites, and *p*-coumaric acid has the lowest. Thus, chlorogenic acid interacts strongly with the adsorbent occupying the active sites in all polymers. Similarly, *p*-coumaric acid interacts weakly with the polymer, promoting the adsorption of other molecules. Consequently, the performance of P1, P3, and P4 is compromised, making P2 a suitable choice for the purification of target acids from a mixture.





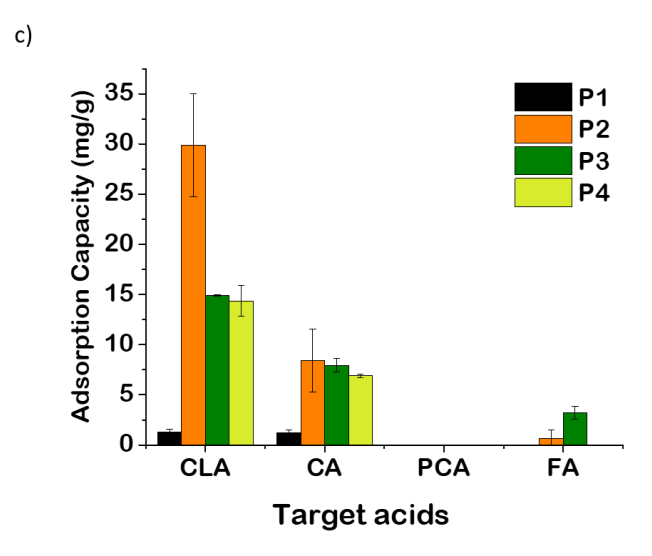


Figure 3: a) Single component adsorption capacity of polymers made of different functional monomers with chlorogenic acid (template) and EDGMA (crosslinker) for 1 mg/mL chlorogenic acid in DMF at 298 K for 2 h. Multicomponent adsorption capacity of polymers made of different b) monomer and c) template from a mixture containing an equal concentration of chlorogenic, caffeic, *p*-coumaric, and ferulic acid at 0.1 mg/mL in DMF at 298 K for 2 h. The polymers P1, P2, P3, and P4 are described in Supplementary Table 8. 2,6-DAP, *o*-AP, 2,6-DAP, *o*-AP, *o*-PHY, ITA, HEM, ACY, and 4-VP stand for 2,6-diaminopyridine, *o*-aminophenol, *o*-phenylenediamine, itaconic acid, 2-hydroxyethyl methacrylate, acrylamide, and 4-vinyl pyridine, respectively. CLA, CA, PCA, and FA are chlorogenic acid, caffeic acid, *p*-coumaric acid, and ferulic acid.

Characterization of the Synthesized Polymers

We characterized the morphology of the synthesized polymers using SEM (Supplementary Figure 3) and confirmed the molecular structure using FTIR. The IR spectrum (Figure 4a)

shows the itaconic acid characteristic peaks at 1721 cm⁻¹ (C=O stretching band) and 1393 cm⁻¹ ¹ (OH bending) and crosslinker characteristic peak at 1150 cm⁻¹ (C-O-C stretching). [68–70] The presence of the C-C stretching band at 1450 cm⁻¹ provides evidence for crosslinked structure and formation of the target polymer. SEM for imprinted (Figure 4b) and nonimprinted polymer (Figure 4c) (functional monomer:itaconic acid) depict porous materials confirming their suitability as adsorbents. The successful removal of the template chlorogenic acid was verified using HPLC analysis (see methods), as similar functional groups (-COOH, -OH) limit the identification of chlorogenic acid in the polymer using IR. The polymer's swelling ratio is 0.09 ± 0.02 , 0.16 ± 0.08 , and 0.50 ± 0.01 in water, ethanol, and DMF. The low swelling ratio of the polymer provides strong evidence for having a highly crosslinked structure. The BET surface area of the imprinted and non-imprinted polymer is 152.22 and 235.51 m²/g, with average pore sizes of 10.64 and 10.28 nm. The polymers are mesoporous with a Type IV adsorption isotherm indicating the formation of a monolayer followed by multilayer adsorption (see below). The TGA curve for the polymer with itaconic acid (see Supplementary Figure 4) shows ~2 wt% loss until 136 °C, possibly due to volatilization of absorbed moisture or THF. The polymer gradually loses another ~4 wt% between 136 °C and 300 °C, corresponding to the removal of the remaining functional monomer (a boiling point of 268 °C) and crosslinker (boiling point of 235 °C). We observe a steep loss at higher temperatures (300 – 500 °C), indicating polymer degradation. Hence, the synthesized polymer is thermally stable up to 300 °C under our conditions.

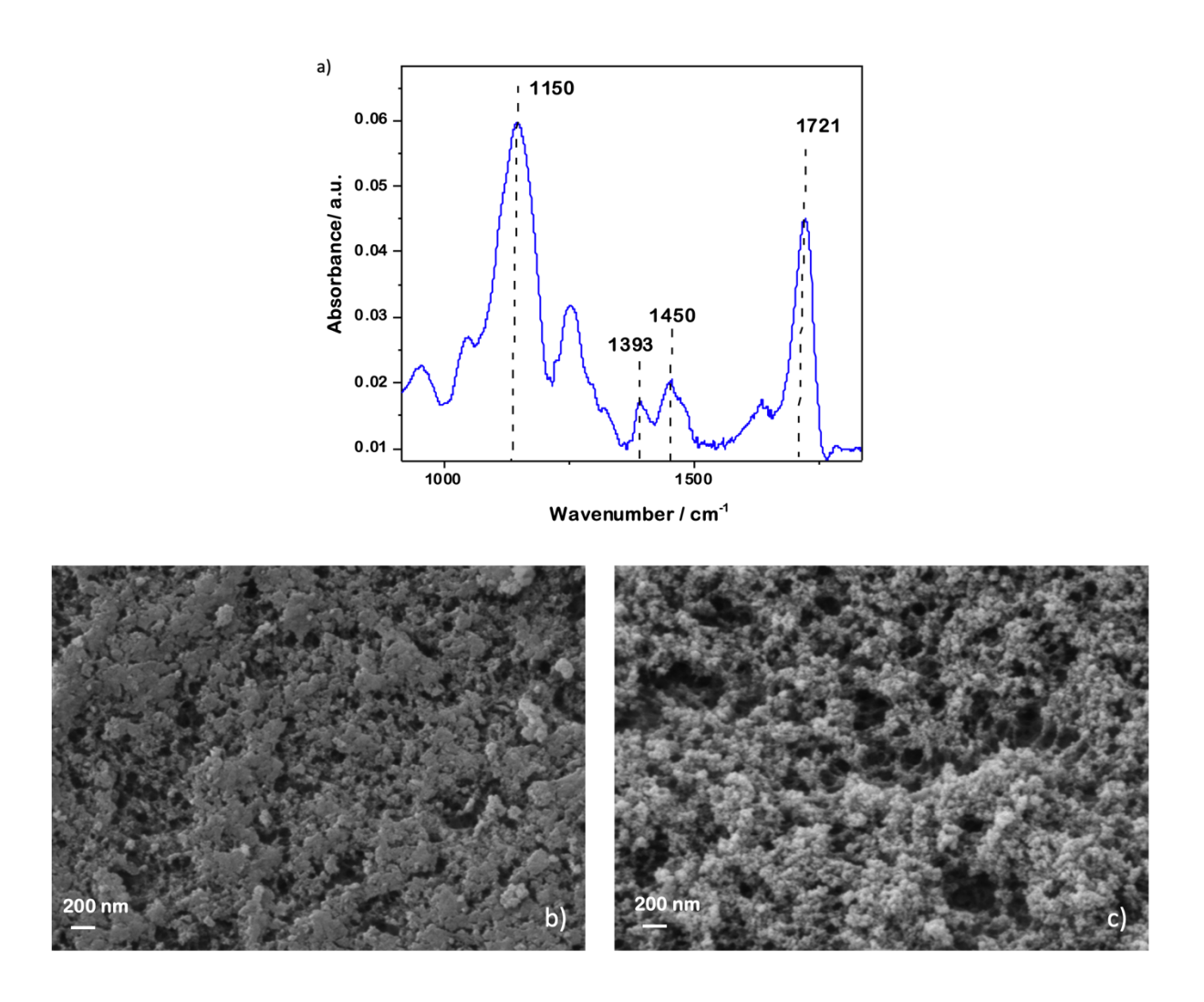


Figure 4: a) FTIR spectrum of chlorogenic acid imprinted polymer with functional monomer itaconic acid and THF as the solvent at 1:3 monomer to crosslinker ratio. Scanning electron micrographs of b) imprinted polymer and c) non-imprinted polymer with itaconic acid as the functional monomer.

Range of Selective Adsorption and P2 Selectivity for Mixtures

The P2 batch adsorption with time was estimated to determine the system equilibrium (see Supplementary Figure 5a). It attains equilibrium in 2 h with minimal variations thereafter.

The solvent-polymer interaction dictates adsorption and potentially causes the observed variation (see below). The Redlich-Peterson model adequately describes the adsorption of chlorogenic acid on P2 (Supplementary Figure 5b), indicating monolayer followed by multilayer adsorption consistent with the BET isotherm. The exponent of 0.6 (see Supplementary Table 9 for regression coefficients) indicates a relatively heterogeneous surface.

We measured P2's efficacy for a concentrated mixture of target acids. The polymer is highly selective to chlorogenic acid at concentrations as low as 0.1 µg/mL mixture of acids in DMF (see below). On the contrary, P2's selectivity decreases steeply between 0.1 to 5 mg/mL and plateaus at higher concentrations (Figure 5a). We believe that non-selective pores on P2, due to its heterogeneous surface, cause this behavior.[71,72] The selective pores of P2 get occupied at lower analyte concentrations leaving only non-selective pores. These pores behave like a non-imprinted polymer, showing no preference for any analyte. P2 is still highly efficient at low concentrations extracted from FW (~ 0.01 to 20 μg/mL). A stagewise adsorption process with an extraction unit (see process flow diagram in Supplementary Figure 6) using P2 can provide high purity of target compounds at each stage. Future work on synthesizing homogeneously imprinted polymers using controlled radical or covalent polymerization would be valuable.[73] Further, controlled/living radical polymerization techniques, such as reversible addition-fragmentation chain transfer, iniferter, and atom transfer radical polymerization, provide efficient alternatives to the traditionally time-intensive free radical polymerization.[74–76]

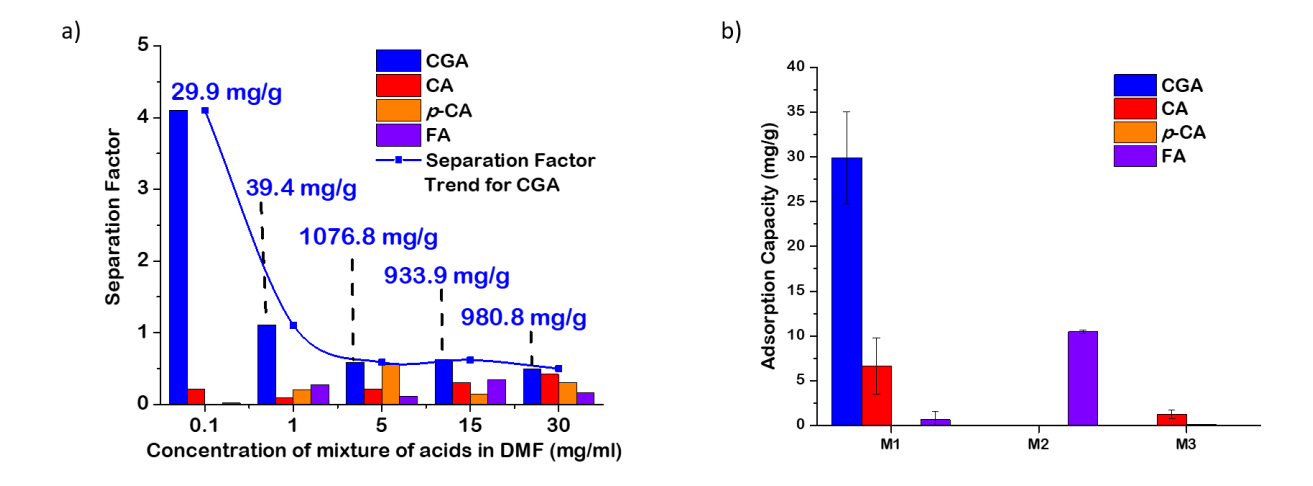


Figure 5: a) Separation factor of imprinted polymer P2 vs. concentration of a solution containing an equal weight percent mixture of acids (chlorogenic, caffeic, *p*-coumaric, and ferulic acid) in DMF at 298 K for 2 h. The line is a visual guide only, and the data labels represent chlorogenic acid adsorption capacity (mg/g). b) P2 adsorption capacity in equal concentration (0.1 mg/mL) mixtures of different target compounds in DMF 298 K, and 2 h. M1 is a mixture containing an equal concentration of chlorogenic, caffeic, *p*-coumaric, and ferulic acid at 0.2 mg/mL. M2 is a mixture containing an equal concentration of caffeic, *p*-coumaric, and ferulic acid at 0.2 mg/mL. M3 is a mixture containing an equal concentration mixture of caffeic and *p*-coumaric acid at 0.2 mg/mL. CGA, CA, *p*-CA, and FA denote chlorogenic, caffeic, *p*-coumaric, and ferulic acid.

Further, we examined P2's selectivity in mixtures in stagewise adsorption (Figure 5b). We prepared three standard mixtures (M1, M2, and M3) of different components. When all four phenolics are present (M1), P2 displays the highest selectivity toward chlorogenic acid. It is selective to ferulic acid when only three phenolics except chlorogenic acid are present (M2).

When only *p*-coumaric and caffeic acid are present, it is selective to the latter. The P2's selectivity in mixtures with the highest adsorbing acid removed each time is:

chlorogenic acid > ferulic acid > caffeic acid > *p*-coumaric acid

P2's performance depends on the polarity and HB interactions with the adsorbate. As discussed above, chlorogenic and *p*-coumaric acid have the most and least HB sites, respectively. Due to this and chlorogenic acid being the imprinted molecule, it is favored by P2. Similarly, P2 has the lowest selectivity towards *p*-coumaric acid. Structurally, ferulic acid has an HB acceptor group (O-CH₃), while caffeic acid has an HB donor group (O-H). The HB donor active site and itaconic acid interact more strongly with the ferulic acid than the caffeic acid. Hence, P2 can purify the target compounds consecutively due to its responsiveness to different functionalities.

P2's Performance and Stability in DMF and Common Extraction Solvents

Ethanol and water are common solvents used for extracting bioactive compounds from FW, plants, and biomass.[77,78] DMF is a polar aprotic solvent with good HB acceptor character that efficiently extracts target compounds from the aforestated feedstocks. Thus, we tested P2's performance and stability in these three solvents to evaluate its scope for diverse applications. Water provides the highest single-component adsorption capacity

 $(307.36 \pm 33.02 \text{ mg/g})$ of chlorogenic acid (1 mg/mL) on P2, followed by DMF $(148.38 \pm 6.58 \text{ mg/g})$, and ethanol $(85.39 \pm 1.46 \text{ mg/g})$. P2 displays nominal separation efficiency for all acids during multicomponent adsorption in water with the highest selectivity towards p-coumaric acid (separation factor = 1.4) (see Supplementary Table 10 for separation factors in water and ethanol). It selectively separates chlorogenic acid from a multicomponent mixture in ethanol (separation factor = 8.72) (Figure 6a). Therefore, P2 has superior performance in ethanol, followed by DMF, and lastly, water.

The solvent effect on the adsorbent separation efficiency is well-studied in the literature.[22,79–82] The hydrophobic/hydrophilic interaction of the extraction solvent with the adsorbent affects its performance. When adsorption is carried out in the solvent used for imprinting, the adsorbent's binding efficiency is enhanced due to a stable cavity structure. [83] Conversely, the polymer solvation in other solvents can lead to unstable conformations and changes in the cavity structure. We utilized FT-IR to study the interactions of the selected solvents with P2 (see Supplementary Figure 7 for P2 interaction with water and ethanol). Ethanol and water have strong HB character due to hydroxyls, which limits the identification of HB with IR. For P2 in DMF (Figure 6b), we observe that the C=O band of DMF [84,85] at 1660 cm⁻¹ shifts to lower wavenumber (~10 cm⁻¹), and a new O-H stretching band at 3465 cm⁻¹ appears. [68,86,87] A similar peak shift (~7 cm⁻¹) of the C=O band and the appearance of the O-H band (3260 cm⁻¹) is seen when mixtures of DMF and chlorogenic acid are analyzed (see Supplementary Figure 7e). This indicates that the C=O band of DMF accepts HB from P2 (-COOH, -OH) or chlorogenic acid, which can influence P2's cavity

structure and performance. Alternatively, polymer swelling can alter the cavity structure leading to low selectivity. The polymer swelling (see above) is relatively low due to the high crosslinker amount that governs the pore size and selectivity. [88] This work used the 1:3 monomer-to-crosslinker ratio widely accepted for non-covalent imprinting. [89,90] A further increase in the crosslinker amount can lead to reduced pore size and selectivity. [91,92] The inherent HB and high swelling ratio of P2 in DMF caused the observed fluctuations over time (Supplementary Figure 5), leading to large error bars in adsorption capacity (see Supplementary Information for details). The weak interaction of P2 with ethanol compared to DMF, evidenced by its lower swelling ratio in ethanol is likely responsible for the observed higher selectivity due to minimal changes in the cavity structure. Further, both P2 and target compounds exhibit weak interactions with water. As a result, these compounds tend to adsorb on P2 instead, making separation less selective in water.

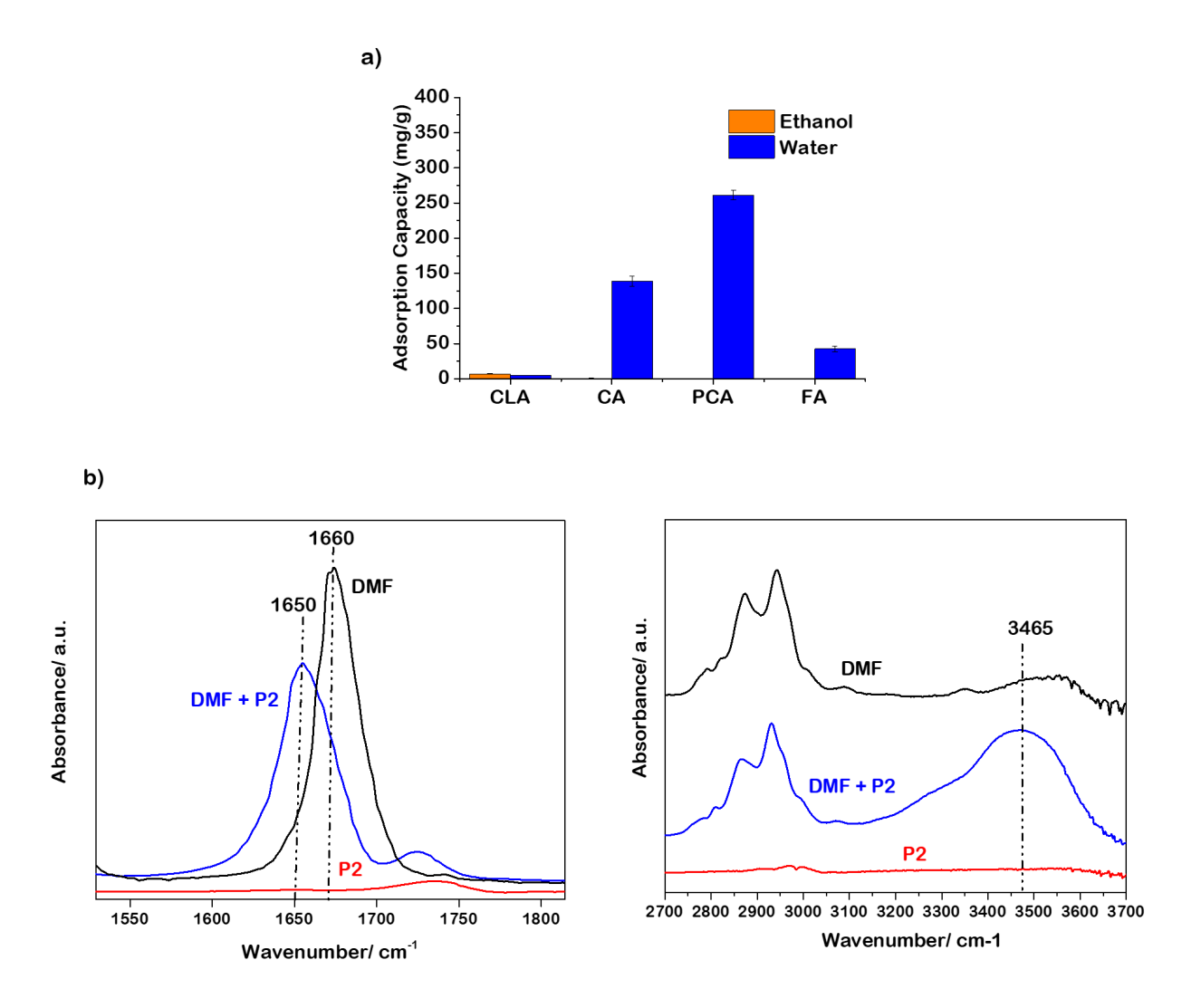


Figure 6: a) Multicomponent adsorption capacity of imprinted polymer P2 for an equal concentration (0.1 mg/mL) mixture of acids (chlorogenic, caffeic, *p*-coumaric and ferulic acid) in ethanol and water at 298 K for 2 h and 30 min, respectively. b) FTIR absorbance of saturated mixture of DMF and polymer P2. CLA, CA, PCA, and FA stand for chlorogenic acid, caffeic acid, *p*-coumaric acid and ferulic acid.

Reusability

We tested P2 for its reusability. P2 was collected after batch adsorption up to three times, washed with methanol, and dried under vacuum. Its adsorption capacity increased with every recycle, but the selectivity decreased (Figure 7). It still provides nominal selectivity for up to three recycles. The separation factor reduces by ~50% after the first recycling and ~20% in the subsequent cycles. As discussed above, P2 has limited stability in DMF and, thus, loses selective pores. The polymer reuse could also rupture the selective pores due to the lack of P2's stability in different solvents.

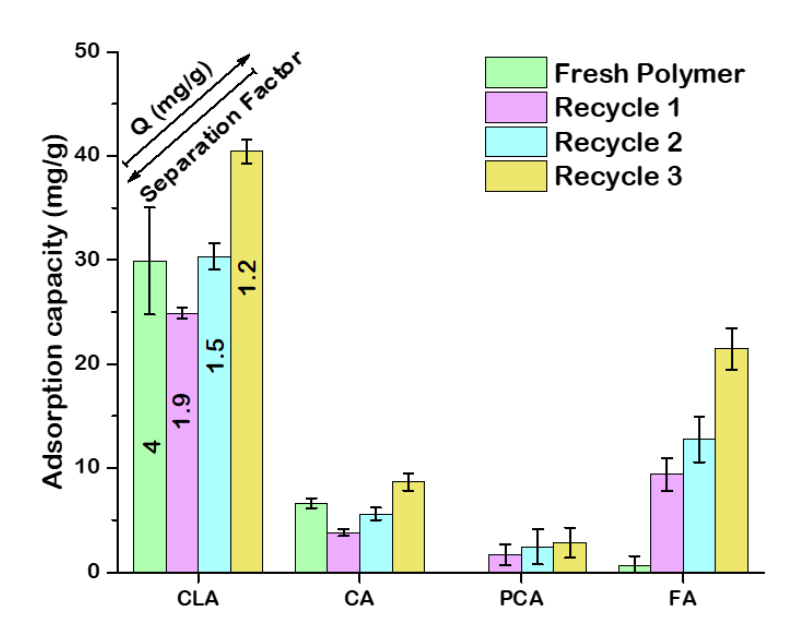


Figure 7: Multicomponent adsorption capacity of the fresh imprinted polymer P2 and spent polymer P2 recycled up to three times from a mixture containing an equal concentration of chlorogenic, caffeic, *p*-coumaric, and ferulic acid at 0.1 mg/mL in DMF at 298 K for 2 h. Q is the adsorption capacity in mg/g. CLA, CA, PCA, and FA stand for chlorogenic acid, caffeic acid, *p*-coumaric acid and ferulic acid.

Application to real FW

We prepared potato peel waste (PPW) and spent coffee bean waste (CW) extracts in DMF (see methods) to examine P2's performance. We detected all four target compounds in PPW and only three (except *p*-coumaric acid) in CW (see the concentration of target acids in Supplementary Table 11) using UPLC-MS (see Methods, see UPLC chromatograms in Supplementary Figure 12). P2 selectively purifies 86% and 92% chlorogenic acid in one cycle from PPW and coffee waste due to higher concentrations of chlorogenic acid in the selected feedstocks (Figure 8). P2 can provide an even higher purity of chlorogenic acid (>99%) in subsequent cycles.

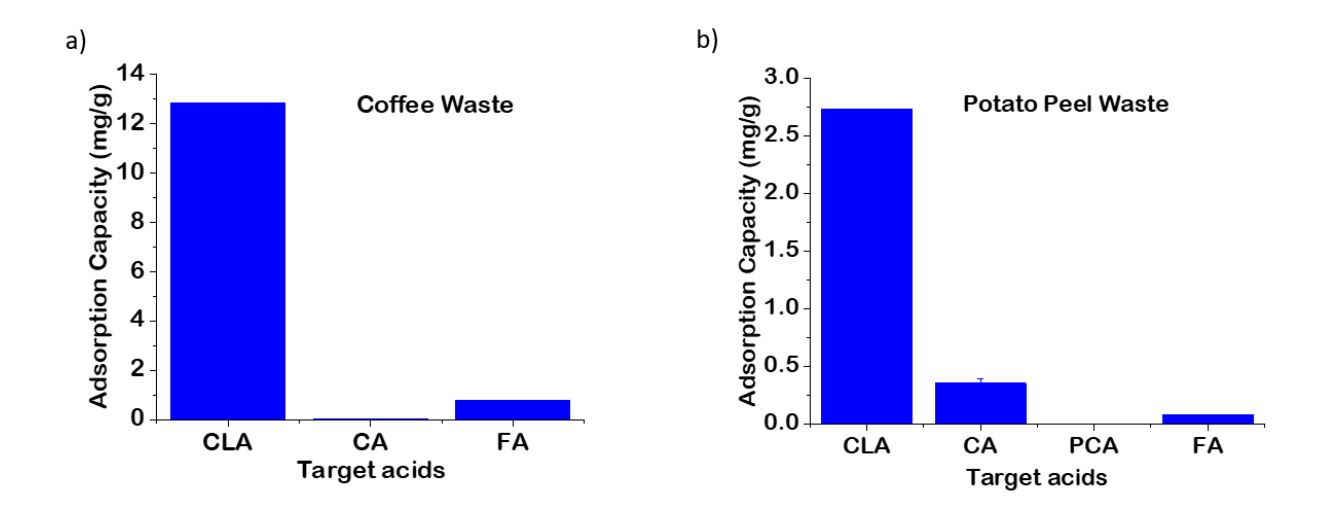


Figure 8: P2 performance in multicomponent mixtures extracted at 298 K for 2 h from a) coffee waste and b) potato peel waste. CLA, CA, PCA, and FA stand for chlorogenic acid, caffeic acid, p-coumaric acid and ferulic acid.

Lab scale economic and carbon footprint analysis

Various grades of chlorogenic acid are produced commercially and priced based on purity. The 45% and 50% pure chlorogenic acid is valued at \$0.16[16] and \$0.28[93] per gram, whereas pure chlorogenic acid per USP reference standard[94] and 95% pure chlorogenic acid[95] cost \$7,220/g and \$122/g.

We estimated the cost for producing pure chlorogenic acid from spent coffee beans using P2 with a simple lab-scale economic analysis as (CGA is chlorogenic acid) (see Supplementary Figure 8 for the process flow diagram):

Cost of purifying CGA = cost of $(CGA \ extraction + P2 \ synthesis + Separation)$

Burniol-Figols et al. estimated the cost of extracting chlorogenic acid from spent coffee beans using 60% (v/v) ethanol at a solid-to-liquid ratio of 1:10 and 70 °C for 40 min at \$0.13/g.[96] One lab-scale P2 synthesis reaction and separation cycle gives ~ 4 g polymer and 92% pure chlorogenic acid. The detailed calculations are provided in SI (Supplementary Table 12 and 13). We estimate the cost of obtaining 1 g of pure chlorogenic acid at \$11.00/g. Hence, the proposed strategy provides at least 11 times more economic value than the commercially available product at 95% purity grade.

Further, we evaluated the carbon footprint of the proposed technology (see Supplementary Figure 8) and contrasted it with Kao Corporation's (see Supplementary Figure 1). The proposed approach offers three distinctions (Table 1): a) choice of feedstock, b) adsorbent, and c) recovery method. The Kao corporation utilizes raw coffee beans with nearly the same

chlorogenic acid amount found in the waste and a higher carbon footprint.[97,98] We assume both methods' adsorbent synthesis carbon emissions are roughly equivalent and compare the emissions from the monomer production. SP-207 adsorbent consists of a brominated styrene-divinylbenzene matrix synthesized from benzene (monomer). Our proposed method incorporates ultrasonic desorption and vacuum concentration as the recovery process, whereas Kao Corporation's recovery process involves column washing followed by vacuum concentration. Consequently, the proposed process reduces carbon emissions by at least ~95% (see Supplementary Information and Table 14 for detailed calculations) by utilizing waste-derived feedstock and monomer and fosters a circular economy to produce high-value chemicals.

Table 1: Carbon footprint of the industrial and proposed technology for extraction and purification of chlorogenic acid.

	Kao	Corporation	Proposed Tech	nology Carbon
Metric	Technology Footprint		Footprint	
	(kg CO2e)		(kg CO2e)	
	Raw coffee	14-16/kg green	Spent coffee	
Feedstock	beans	coffee powder	beans	0
Monomer	SP-207	1.76/kg	P2	0/kg itaconic

Production		benzene		acid
			Batch	
Recovery	Elution on	0.06/kWh	ultrasonic	0.03/kWh
	column		desorption	
			desorption	
	Per g		Per g	
Total	chlorogenic	3.32-3.36	chlorogenic	0.07
	acid		acid	

Conclusions

Extracting high commercial-value bioactive compounds, such as phenolic acids, from FW and non-food biomass is an attractive method to repurpose FW. However, the separation and downstream purification of the extracted compounds is challenging. In the current work, molecular imprinted polymers are synthesized to selectively separate the target phenolic acid compounds. We used HSPiP to screen 13 porogenic solvents and 28 monomers and identified THF as the best solvent for polymer synthesis. Experimental investigations revealed that itaconic acid stands out as an efficient and green alternative, providing the highest separation factor for chlorogenic acid compared to previous studies. The selectivity of the optimized polymer (P2) is chlorogenic acid > ferulic acid > caffeic acid > p-coumaric acid. Further, P2 is selective up to 1 mg/mL equal concentration acids mixture in DMF, which is much higher

than in FW, offering a broader range of operations for the polymer and extending its utility beyond traditional analytical applications. The efficacy of this approach is influenced by the extraction solvent employed, as observed in previous studies. Thus, we broadened our investigation by evaluating its efficiency in three distinct extraction solvents in contrast to the conventional single-solvent studies. Ethanol provides the highest separation factor for chlorogenic acid, followed by DMF, and then water. We utilized IR to understand how P2 interacts with different solvents. The high swelling ratio in DMF indicates the possible collapse of selective pores. Thus, P2's recyclability is compromised, encouraging the development of better fabrication methods to produce stable polymers. Its application to a real FW reveals successful extraction of up to 92% and 86% pure chlorogenic acid from coffee beans and potato peel waste, respectively. We compared the proposed method for chlorogenic acid production with a patented industrial process. The proposed technology provides ~11 times more economic value and at least 95% lesser carbon emissions. The application of waste-derived monomer and feedstock assists in offsetting carbon emissions and drives circularity.

Author Contributions

Y.G. and D.G.V. designed the project. Y.G. conceived the project idea, conducted HSPiP and COSMO-RS calculations and carried out all experiments. L. E. B. helped in polymer synthesis initially and performed TGA and swelling ratio studies. V.V. conducted FTIR to study solvent-polymer interactions. All authors contributed to relevant data analysis. Y.G. and

D.G.V. wrote the manuscript with input from S.S. D.G.V., S.S. and L.K. supervised the project.

Acknowledgement

This work was supported by the National Science Foundation (NSF GCR CMMI 1934887).

The authors acknowledge the University of Delaware's Advanced Material Characterization

Laboratory (AMCL) for the DSC and TGA instruments, the Mass Spectrometry Facility, and
the Nanofabrication Facility for the FIB-SEM instrument.

References

- [1] H. Forbes, T. Quested, C. O'Connor, Food Waste Index Report, 2021.
- [2] C. Zhang, H. Su, J. Baeyens, T. Tan, Reviewing the anaerobic digestion of food waste for biogas production, Renewable and Sustainable Energy Reviews. 38 (2014) 383–392. https://doi.org/10.1016/j.rser.2014.05.038.
- [3] A. Cerda, A. Artola, X. Font, R. Barrena, T. Gea, A. Sánchez, Composting of food wastes: Status and challenges, Bioresour Technol. 248 (2018) 57–67. https://doi.org/10.1016/j.biortech.2017.06.133.
- [4] T.P.T. Pham, R. Kaushik, G.K. Parshetti, R. Mahmood, R. Balasubramanian, Food waste-to-energy conversion technologies: Current status and future directions, Waste Management. 38 (2015) 399–408. https://doi.org/10.1016/j.wasman.2014.12.004.
- [5] M. Eriksson, J. Spångberg, Carbon footprint and energy use of food waste management options for fresh fruit and vegetables from supermarkets, Waste Management. 60 (2017) 786–799. https://doi.org/10.1016/j.wasman.2017.01.008.
- [6] W. Wang, P. Xiong, H. Zhang, Q. Zhu, C. Liao, G. Jiang, Analysis, occurrence, toxicity and environmental health risks of synthetic phenolic antioxidants: A review, Environ Res. 201 (2021) 111531. https://doi.org/10.1016/j.envres.2021.111531.
- [7] R. Liu, S.A. Mabury, Synthetic Phenolic Antioxidants: A Review of Environmental Occurrence, Fate, Human Exposure, and Toxicity, Environ Sci Technol. 54 (2020) 11706–11719. https://doi.org/10.1021/acs.est.0c05077.

- [8] S.C. Lourenço, M. Moldão-Martins, V.D. Alves, Antioxidants of natural plant origins: From sources to food industry applications, Molecules. 24 (2019) 4132. https://doi.org/10.3390/molecules24224132.
- [9] O. Taofiq, A.M. González-Paramás, M.F. Barreiro, I.C.F.R. Ferreira, D.J. McPhee, Hydroxycinnamic acids and their derivatives: Cosmeceutical significance, challenges and future perspectives, a review, Molecules. 22 (2017) 281. https://doi.org/10.3390/molecules22020281.
- [10] Market Growth Reports, Chlorogenic Acid Market Size In 2022: New Technological Trend & Development with Top Key Players, Industry Analysis by Top Manufactures, Product Demand Forecast Till 2026, The Express Wire. (2022). https://www.marketwatch.com/press-release/chlorogenic-acid-market-size-in-2022-new-technological-trend-development-with-top-key-players-industry-analysis-by-top-manufactures-product-demand-forecast-till-2026-124-report-pages-2022-08-09 (accessed October 31, 2022).
- [11] Ferulic Acid Market (By Type: Synthesis, Natural; By Application: Cosmetic, Pharmaceutical Intermediates, Others; By Packaging: Interior Packaging, Exterior Packaging) Global Industry Analysis, Size, Share, Growth, Trends, Regional Outlook, and Forecast 2022-2030, Precedence Research. (2022). https://www.precedenceresearch.com/ferulic-acid-market.
- [12] NutraGreen, Green Coffee bean Extract Chlorogenic Acids, NutraGreen. (2022). https://www.nutragreenbio.com/product/green-coffee-bean-extract-chlorogenic-acids.
- [13] Euromed, Artichoke Extracts, 2022. https://www.euromedgroup.com/product-details/artichoke-leaf-cynara-scolymus-l/.
- [14] Cymbio Pharma, Herbal Extracts, Cymbio Pharma. (2022). https://www.cymbio.co.in/products/herbal-extracts/.
- [15] Flavour Trove, Human Health Care , Flavour Trove. (2022). https://www.flavourtrove.com/products%20-%20human%20health.html.
- [16] Applied Food Sciences, Green Coffee Extract, Applied Food Sciences. (2022). https://appliedfoods.com/ingredients/gca/.
- [17] M. Fukuda, H. Takahashi, A. Konishi, Method of producing chlorogenic acid composition, US 8,309,150 B2, 2012.
- [18] M.N. Peyrat-Maillard, M.E. Cuvelier, C. Berset, Antioxidant Activity of Phenolic Compounds in 2,2'-Azobis (2-amidinopropane) Dihydrochloride (AAPH)-Induced

- Oxidation: Synergistic and Antagonistic Effects, JAOCS, Journal of the American Oil Chemists' Society. 80 (2003) 1007–1012. https://doi.org/10.1007/s11746-003-0812-z.
- [19] P.C. Hugo, J. Gil-Chávez, R.R. Sotelo-Mundo, J. Namiesnik, S. Gorinstein, G.A. González-Aguilar, Antioxidant interactions between major phenolic compounds found in "Ataulfo" mango pulp: Chlorogenic, gallic, protocatechuic and vanillic acids, Molecules. 17 (2012) 12657–12664. https://doi.org/10.3390/molecules171112657.
- [20] S. Wang, K.A. Meckling, M.F. Marcone, Y. Kakuda, R. Tsao, Synergistic, additive, and antagonistic effects of food mixtures on total antioxidant capacities, J Agric Food Chem. 59 (2011) 960–968. https://doi.org/10.1021/jf1040977.
- [21] K. Ramalakshmi, I. Rahath Kubra, L. Jagan Mohan Rao, Antioxidant potential of low-grade coffee beans, Food Research International. 41 (2008) 96–103. https://doi.org/10.1016/j.foodres.2007.10.003.
- [22] A. Ostovan, M. Arabi, Y. Wang, J. Li, B. Li, X. Wang, L. Chen, Greenificated Molecularly Imprinted Materials for Advanced Applications, Advanced Materials. 34 (2022) 2203154. https://doi.org/10.1002/adma.202203154.
- [23] H. Santos, R.O. Martins, D.A. Soares, A.R. Chaves, Molecularly imprinted polymers for miniaturized sample preparation techniques: Strategies for chromatographic and mass spectrometry methods, Analytical Methods. 12 (2020) 894–911. https://doi.org/10.1039/c9ay02227a.
- [24] D. Çimen, N. Bereli, M. Andaç, A. Denizli, Molecularly imprinted cryogel columns for Concanavalin A purification from jack bean extract, Sep Sci Plus. 1 (2018) 454–463. https://doi.org/10.1002/sscp.201800039.
- [25] T. Esteves, F.A. Ferreira, A.T. Mota, Á. Sánchez-González, A. Gil, K.H.S. Andrade, C.A.M. Afonso, F.C. Ferreira, Greener Strategy for Lupanine Purification from Lupin Bean Wastewaters Using a Molecularly Imprinted Polymer, ACS Appl Mater Interfaces. 14 (2022) 18910–18921. https://doi.org/10.1021/acsami.2c02053.
- [26] Y.L. Mustafa, A. Keirouz, H.S. Leese, Molecularly imprinted polymers in diagnostics: accessing analytes in biofluids, J Mater Chem B. 10 (2022) 7418–7449. https://doi.org/10.1039/d2tb00703g.
- [27] S. Basak, R. Venkatram, R.S. Singhal, Recent advances in the application of molecularly imprinted polymers (MIPs) in food analysis, Food Control. 139 (2022) 109074. https://doi.org/10.1016/j.foodcont.2022.109074.
- [28] L.M. Madikizela, P.N. Nomngongo, V.E. Pakade, Synthesis of molecularly imprinted polymers for extraction of fluoroquinolones in environmental, food and biological

- samples, J Pharm Biomed Anal. 208 (2022) 114447. https://doi.org/10.1016/j.jpba.2021.114447.
- [29] R. Tian, Y. Li, J. Xu, C. Hou, Q. Luo, J. Liu, Recent development in the design of artificial enzymes through molecular imprinting technology, J Mater Chem B. 10 (2022) 6590–6606. https://doi.org/10.1039/d2tb00276k.
- [30] R. Liu, A. Poma, Advances in molecularly imprinted polymers as drug delivery systems, Molecules. 26 (2021) 3589. https://doi.org/10.3390/molecules26123589.
- [31] Z. Gu, Y. Dong, S. Xu, L. Wang, Z. Liu, Molecularly Imprinted Polymer-Based Smart Prodrug Delivery System for Specific Targeting, Prolonged Retention, and Tumor Microenvironment-Triggered Release, Angewandte Chemie International Edition. 60 (2021) 2663–2667. https://doi.org/10.1002/anie.202012956.
- [32] Q. Liu, Y. Zhao, J. Pan, B. Van Der Bruggen, J. Shen, A novel chitosan base molecularly imprinted membrane for selective separation of chlorogenic acid, Sep Purif Technol. 164 (2016) 70–80. https://doi.org/10.1016/j.seppur.2016.03.020.
- [33] N. Li, T.B. Ng, J.H. Wong, J.X. Qiao, Y.N. Zhang, R. Zhou, R.R. Chen, F. Liu, Separation and purification of the antioxidant compounds, caffeic acid phenethyl ester and caffeic acid from mushrooms by molecularly imprinted polymer, Food Chem. 139 (2013) 1161–1167. https://doi.org/10.1016/j.foodchem.2013.01.084.
- [34] N. Li, T.B. Ng, J.H. Wong, J.X. Qiao, Y.N. Zhang, R. Zhou, R.R. Chen, F. Liu, Separation and purification of the antioxidant compounds, caffeic acid phenethyl ester and caffeic acid from mushrooms by molecularly imprinted polymer, Food Chem. 139 (2013) 1161–1167. https://doi.org/10.1016/j.foodchem.2013.01.084.
- [35] Yi Hao, Ruixia Gao, Dechun Liu, Gaiyan He, Yuhai Tang, Zengjun Guo, Selective extraction and determination of chlorogenic acid in fruit juices using hydrophilic magnetic imprinted nanoparticles, Food Chem. (2016) 215–222. https://doi.org/10.1016/j.foodchem.2016.01.004.
- [36] Yayun Zhao, Yuhai Tang, Jun He, Yuan Xu, Ruixia Gao, Junjie Zhang, Tie Chong, Li Wang, Xiaoshuang Tang, Surface imprinted polymers based on amino-hyperbranched magnetic nanoparticles for selective extraction and detection of chlorogenic acid in Honeysuckle tea, Talanta. 181 (2018) 271–277. https://doi.org/10.1016/j.talanta.2018.01.037.
- [37] Y. Gupta, S. Bhattacharyya, D.G. Vlachos, Extraction of valuable chemicals from food waste via computational solvent screening and experiments, Sep Purif Technol. 316 (2023). https://doi.org/10.1016/j.seppur.2023.123719.

- [38] P. Khuwijitjaru, J. Plernjit, B. Suaylam, S. Samuhaseneetoo, R. Pongsawatmanit, S. Adachi, Degradation kinetics of some phenolic compounds in subcritical water and radical scavenging activity of their degradation products, Canadian Journal of Chemical Engineering. 92 (2014) 810–815. https://doi.org/10.1002/cjce.21898.
- [39] G.P. Rizzi, L.J. Boekley, Observation of Ether-Linked Phenolic Products during Thermal Degradation of Ferulic Acid in the Presence of Alcohols, J Agric Food Chem. 40 (1992) 1666–1670. https://doi.org/10.1021/jf00021a037.
- [40] J.K. Moon, T. Shibamoto, Formation of volatile chemicals from thermal degradation of less volatile coffee components: Quinic acid, caffeic acid, and chlorogenic acid, J Agric Food Chem. 58 (2010) 5465–5470. https://doi.org/10.1021/jf1005148.
- [41] R.J. Lehnert, R. Schilling, Accuracy of molar solubility prediction from hansen parameters. An exemplified treatment of the bioantioxidant l-ascorbic acid, Applied Sciences (Switzerland). 10 (2020) 4266. https://doi.org/10.3390/app10124266.
- [42] S. Wang, J.M. Stubbs, J.I. Siepmann, S.I. Sandler, Effects of conformational distributions on sigma profiles in COSMO theories, Journal of Physical Chemistry A. 109 (2005) 11285–11294. https://doi.org/10.1021/jp053859h.
- [43] C. Michailof, P. Manesiotis, C. Panayiotou, Synthesis of caffeic acid and phydroxybenzoic acid molecularly imprinted polymers and their application for the selective extraction of polyphenols from olive mill waste waters, J Chromatogr A. 1182 (2008) 25–33. https://doi.org/10.1016/j.chroma.2008.01.001.
- [44] D. Fan, H. Li, S. Shi, X. Chen, Hollow molecular imprinted polymers towards rapid, effective and selective extraction of caffeic acid from fruits, J Chromatogr A. 1470 (2016) 27–32. https://doi.org/10.1016/j.chroma.2016.10.006.
- [45] Y. García, B.A. Úsuga, C.H. Campos, J.B. Alderete, V.A. Jiménez, NanoMIPs Design for Fucose and Mannose Recognition: A Molecular Dynamics Approach, J Chem Inf Model. 61 (2021) 2048–2061. https://doi.org/10.1021/acs.jcim.0c01446.
- [46] K. Bartold, Z. Iskierko, P. Borowicz, K. Noworyta, C.Y. Lin, J. Kalecki, P.S. Sharma, H.Y. Lin, W. Kutner, Molecularly imprinted polymer-based extended-gate field-effect transistor (EG-FET) chemosensor for selective determination of matrix metalloproteinase-1 (MMP-1) protein, Biosens Bioelectron. 208 (2022) 114203. https://doi.org/10.1016/j.bios.2022.114203.
- [47] S.L. Moura, L.M. Fajardo, L. dos A. Cunha, M.D.P.T. Sotomayor, F.B.C. Machado, L.F.A. Ferrão, M.I. Pividori, Theoretical and experimental study for the biomimetic recognition of levothyroxine hormone on magnetic molecularly imprinted polymer, Biosens Bioelectron. 107 (2018) 203–210. https://doi.org/10.1016/j.bios.2018.01.028.

- [48] M. Arabi, A. Ostovan, A.R. Bagheri, X. Guo, L. Wang, J. Li, X. Wang, B. Li, L. Chen, Strategies of molecular imprinting-based solid-phase extraction prior to chromatographic analysis, TrAC Trends in Analytical Chemistry. 128 (2020) 115923. https://doi.org/10.1016/j.trac.2020.115923.
- [49] L. Chen, X. Wang, W. Lu, X. Wu, J. Li, Molecular imprinting: Perspectives and applications, Chem Soc Rev. 45 (2016) 2137–2211. https://doi.org/10.1039/c6cs00061d.
- [50] M. Dutkiewicz, Classification of Organic Solvents based on Correlation between Dielectric β Parameter and Empirical Solvent Polarity Parameter, J. Chem. Soc. Faraday Trans. 86 (1990) 2237–2241. https://doi.org/10.1039/FT9908602237.
- [51] J. Wyman Jr., Dielectric Constants of Polar Solutions, J Am Chem Soc. 56 (1934) 536–544. https://doi.org/10.1021/ja01318a008.
- [52] X. Luo, C. Li, Y. Duan, H. Zhang, D. Zhang, C. Zhang, G. Sun, X. Sun, Molecularly imprinted polymer prepared by Pickering emulsion polymerization for removal of acephate residues from contaminated waters, J Appl Polym Sci. 133 (2016) 1–11. https://doi.org/10.1002/app.43126.
- [53] S.L. Moura, L.M. Fajardo, L. dos A. Cunha, M.D.P.T. Sotomayor, F.B.C. Machado, L.F.A. Ferrão, M.I. Pividori, Theoretical and experimental study for the biomimetic recognition of levothyroxine hormone on magnetic molecularly imprinted polymer, Biosens Bioelectron. 107 (2018) 203–210. https://doi.org/10.1016/j.bios.2018.01.028.
- [54] J. Yao, X. Li, W. Qin, Computational design and synthesis of molecular imprinted polymers with high selectivity for removal of aniline from contaminated water, Anal Chim Acta. 610 (2008) 282–288. https://doi.org/10.1016/j.aca.2008.01.042.
- [55] L. Peng, Y. Wang, H. Zeng, Y. Yuan, Molecularly imprinted polymer for solid-phase extraction of rutin in complicated traditional Chinese medicines, Analyst. 136 (2011) 756–763. https://doi.org/10.1039/c0an00798f.
- [56] D. Elfadil, A. Lamaoui, F. Della Pelle, A. Amine, D. Compagnone, Molecularly imprinted polymers combined with electrochemical sensors for food contaminants analysis, Molecules. 26 (2021) 4607. https://doi.org/10.3390/molecules26154607.
- [57] M. Gao, Y. Gao, G. Chen, X. Huang, X. Xu, J. Lv, J. Wang, D. Xu, G. Liu, Recent Advances and Future Trends in the Detection of Contaminants by Molecularly Imprinted Polymers in Food Samples, Front Chem. 8 (2020) 616326. https://doi.org/10.3389/fchem.2020.616326.
- [58] N. Li, T.B. Ng, J.H. Wong, J.X. Qiao, Y.N. Zhang, R. Zhou, R.R. Chen, F. Liu, Separation and purification of the antioxidant compounds, caffeic acid phenethyl ester

- and caffeic acid from mushrooms by molecularly imprinted polymer, Food Chem. 139 (2013) 1161–1167. https://doi.org/10.1016/j.foodchem.2013.01.084.
- [59] M. Zhao, H. Shao, J. Ma, H. Li, Y. He, M. Wang, F. Jin, J. Wang, A.M. Abd El-Aty, A. Hacımüftüoğlu, F. Yan, Y. Wang, Y. She, Preparation of core-shell magnetic molecularly imprinted polymers for extraction of patulin from juice samples, J Chromatogr A. 1615 (2020) 460751. https://doi.org/10.1016/j.chroma.2019.460751.
- [60] I.S. Ibarra, J.M. Miranda, I. Pérez-Silva, C. Jardinez, G. Islas, Sample treatment based on molecularly imprinted polymers for the analysis of veterinary drugs in food samples: A review, Analytical Methods. 12 (2020) 2958–2977. https://doi.org/10.1039/d0ay00533a.
- [61] N. Tarannum, S. Khatoon, B.B. Dzantiev, Perspective and application of molecular imprinting approach for antibiotic detection in food and environmental samples: A critical review, Food Control. 118 (2020) 107381. https://doi.org/10.1016/j.foodcont.2020.107381.
- [62] Y. Yuan, Y. Yang, M. Faheem, X. Zou, X. Ma, Z. Wang, Q. Meng, L. Wang, S. Zhao, G. Zhu, Molecularly Imprinted Porous Aromatic Frameworks Serving as Porous Artificial Enzymes, Advanced Materials. 30 (2018) 1800069. https://doi.org/10.1002/adma.201800069.
- [63] S.R. Carter, S. Rimmer, Molecular recognition of caffeine by shell molecular imprinted core-shell polymer particles in aqueous media, Advanced Materials. 14 (2002) 667–670. https://doi.org/10.1002/1521-4095(20020503)14:9<667::AID-ADMA667>3.0.CO;2-3.
- [64] M. Arabi, A. Ostovan, J. Li, X. Wang, Z. Zhang, J. Choo, L. Chen, Molecular Imprinting: Green Perspectives and Strategies, Advanced Materials. 33 (2021) 2100543. https://doi.org/10.1002/adma.202100543.
- [65] K.V. Kumar, S. Gadipelli, B. Wood, K.A. Ramisetty, A.A. Stewart, C.A. Howard, D.J.L. Brett, F. Rodriguez-Reinoso, Characterization of the adsorption site energies and heterogeneous surfaces of porous materials, J Mater Chem A Mater. 7 (2019) 10104–10137. https://doi.org/10.1039/c9ta00287a.
- [66] T. Zhou, L. Ding, G. Che, W. Jiang, L. Sang, Recent advances and trends of molecularly imprinted polymers for specific recognition in aqueous matrix: Preparation and application in sample pretreatment, TrAC - Trends in Analytical Chemistry. 114 (2019) 11–28. https://doi.org/10.1016/j.trac.2019.02.028.

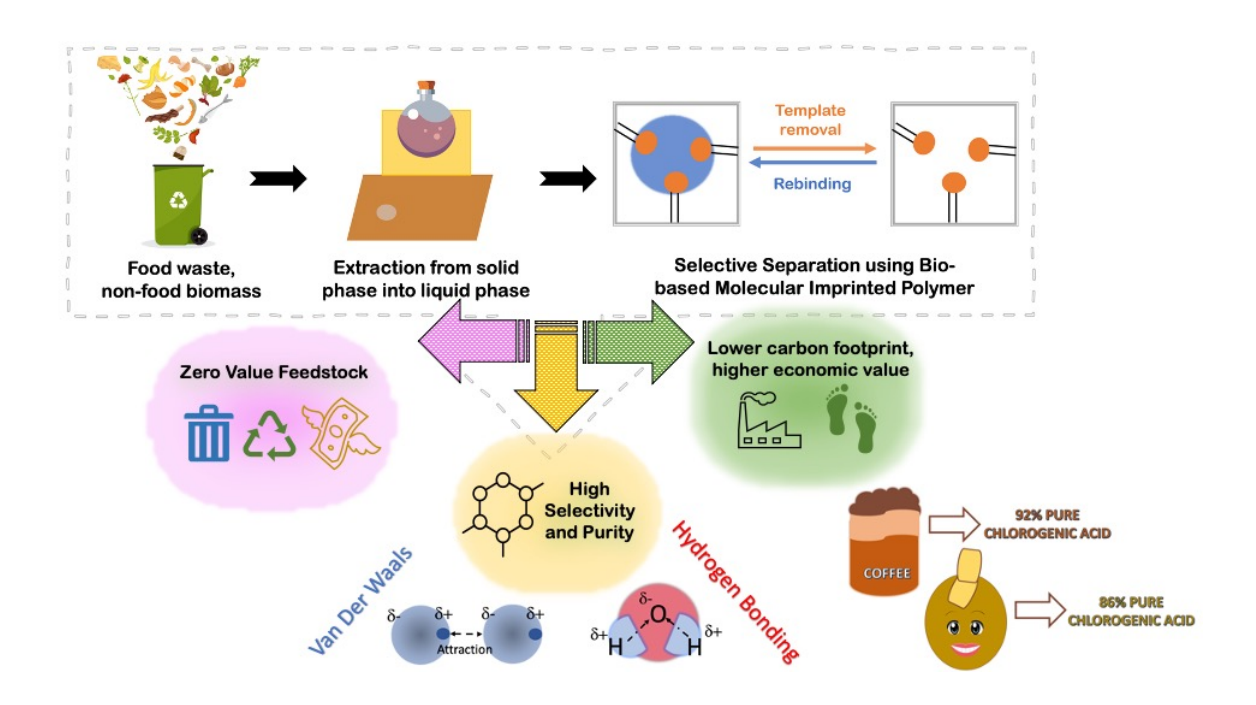
- [67] X. Li, K.H. Row, Preparation of deep eutectic solvent-based hexagonal boron nitride-molecularly imprinted polymer nanoparticles for solid phase extraction of flavonoids, Microchimica Acta. 186 (2019) 1–10. https://doi.org/10.1007/s00604-019-3885-8.
- [68] IR Spectrum Table & Chart, Sigma Aldrich. (2023). https://www.sigmaaldrich.com/US/en/technical-documents/technical-article/analytical-chemistry/photometry-and-reflectometry/ir-spectrum-table (accessed May 31, 2022).
- [69] W. Zhang, X. She, L. Wang, H. Fan, Q. Zhou, X. Huang, J.Z. Tang, Preparation, characterization and application of a molecularly imprinted polymer for selective recognition of sulpiride, Materials. 10 (2017) 1–10. https://doi.org/10.3390/ma10050475.
- [70] G. Marcelo, I.C. Ferreira, R. Viveiros, T. Casimiro, Development of itaconic acid-based molecular imprinted polymers using supercritical fluid technology for pH-triggered drug delivery, Int J Pharm. 542 (2018) 125–131. https://doi.org/10.1016/j.ijpharm.2018.03.010.
- [71] A.M. Rampey, R.J. Umpleby, G.T. Rushton, J.C. Iseman, R.N. Shah, K.D. Shimizu, Characterization of the Imprint Effect and the Influence of Imprinting Conditions on Affinity, Capacity, and Heterogeneity in Molecularly Imprinted Polymers Using the Freundlich Isotherm-Affinity Distribution Analysis, Anal Chem. 76 (2004) 1123–1133. https://doi.org/10.1021/ac0345345.
- [72] R.J. Umpleby, S.C. Baxter, A.M. Rampey, G.T. Rushton, Y. Chen, K.D. Shimizu, Characterization of the heterogeneous binding site affinity distributions in molecularly imprinted polymers, J Chromatogr B Analyt Technol Biomed Life Sci. 804 (2004) 141–149. https://doi.org/10.1016/j.jchromb.2004.01.064.
- [73] T. Zhou, L. Ding, G. Che, W. Jiang, L. Sang, Recent advances and trends of molecularly imprinted polymers for specific recognition in aqueous matrix: Preparation and application in sample pretreatment, TrAC Trends in Analytical Chemistry. 114 (2019) 11–28. https://doi.org/10.1016/j.trac.2019.02.028.
- [74] D. Zhou, L.W. Zhu, B.H. Wu, Z.K. Xu, L.S. Wan, End-functionalized polymers by controlled/living radical polymerizations: Synthesis and applications, Polym Chem. 13 (2022) 300–358. https://doi.org/10.1039/d1py01252e.
- [75] N. Corrigan, K. Jung, G. Moad, C.J. Hawker, K. Matyjaszewski, C. Boyer, Reversible-deactivation radical polymerization (Controlled/living radical polymerization): From discovery to materials design and applications, Prog Polym Sci. 111 (2020) 101311. https://doi.org/10.1016/j.progpolymsci.2020.101311.

- [76] W.A. Braunecker, K. Matyjaszewski, Controlled/living radical polymerization: Features, developments, and perspectives, Progress in Polymer Science (Oxford). 32 (2007) 93–146. https://doi.org/10.1016/j.progpolymsci.2006.11.002.
- [77] A.M. Samarin, H. Poorazarang, N. Hematyar, A. Elhamirad, Phenolics in potato peels: Extraction and utilization as natural antioxidants, World Appl Sci J. 18 (2012) 191–195. https://doi.org/10.5829/idosi.wasj.2012.18.02.1057.
- [78] A. Singh, K. Sabally, S. Kubow, D.J. Donnelly, Y. Gariepy, V. Orsat, G.S.V. Raghavan, Microwave-assisted extraction of phenolic antioxidants from potato peels, Molecules. 16 (2011) 2218–2232. https://doi.org/10.3390/molecules16032218.
- [79] T. Pap, V. Horváth, A. Tolokán, G. Horvai, B. Sellergren, Effect of solvents on the selectivity of terbutylazine imprinted polymer sorbents used in solid-phase extraction, J Chromatogr A. 973 (2002) 1–12. https://doi.org/10.1016/S0021-9673(02)01084-1.
- [80] N.W. Turner, E. V. Piletska, K. Karim, M. Whitcombe, M. Malecha, N. Magan, C. Baggiani, S.A. Piletsky, Effect of the solvent on recognition properties of molecularly imprinted polymer specific for ochratoxin A, Biosens Bioelectron. 20 (2004) 1060–1067. https://doi.org/10.1016/j.bios.2004.06.052.
- [81] D.A. Spivak, Optimization, evaluation, and characterization of molecularly imprinted polymers, Adv Drug Deliv Rev. 57 (2005) 1779–1794. https://doi.org/10.1016/j.addr.2005.07.012.
- [82] C. Gomes, G. Sadoyan, R.C.S. Dias, M.R.P.F.N. Costa, Development of molecularly imprinted polymers to target polyphenols present in plant extracts, Processes. 5 (2017) 72. https://doi.org/10.3390/pr5040072.
- [83] G.J. Maranata, N.O. Surya, A.N. Hasanah, Optimising factors affecting solid phase extraction performances of molecular imprinted polymer as recent sample preparation technique, Heliyon. 7 (2021) e05934. https://doi.org/10.1016/j.heliyon.2021.e05934.
- [84] V.V. Chalapathi, K.V. Ramiah, Normal Vibrations of N,N-Dimethylformamide and N,N-Dimethylacetamide, Proceedings of the Indian Academy of Sciences-Section A. 68 (1968) 109–122. https://doi.org/10.1007/BF03049367.
- [85] M. Malathi, R. Sabesan, S. Krishnan, IR carbonyl band intensity studies in N, N-dimethyl formamide and N, N-dimethyl acetamide on complex formation with phenols, Curr Sci. 86 (2004) 838–842. https://www.jstor.org/stable/24109141 (accessed April 23, 2023).

- [86] E. Libowitzky, Correlation of O-H Stretching Frequencies and O-H O Hydrogen Bond Lengths in Minerals, Hydrogen Bond Research. 1059 (1999) 103–115. https://doi.org/10.1007/978-3-7091-6419-8_7.
- [87] K. Miura, K. Mae, W. Li, T. Kusakawa, F. Morozumi, A. Kumano, Estimation of hydrogen bond distribution in coal through the analysis of OH stretching bands in diffuse reflectance infrared spectrum measured by in-situ technique, Energy and Fuels. 15 (2001) 599–610. https://doi.org/10.1021/ef0001787.
- [88] N.F. Che Lah, A.L. Ahmad, M.H. Mohd Amri, J.Y. Chin, Configuration of molecularly imprinted polymers for specific uptake of pharmaceutical in aqueous media through radical polymerization method, Journal of Polymer Research. 29 (2022) 41. https://doi.org/10.1007/s10965-022-02908-8.
- [89] W. Bi, M. Tian, K.H. Row, Separation of phenolic acids from natural plant extracts using molecularly imprinted anion-exchange polymer confined ionic liquids, J Chromatogr A. 1232 (2012) 37–42. https://doi.org/10.1016/j.chroma.2011.08.054.
- [90] N. Li, T.B. Ng, J.H. Wong, J.X. Qiao, Y.N. Zhang, R. Zhou, R.R. Chen, F. Liu, Separation and purification of the antioxidant compounds, caffeic acid phenethyl ester and caffeic acid from mushrooms by molecularly imprinted polymer, Food Chem. 139 (2013) 1161–1167. https://doi.org/10.1016/j.foodchem.2013.01.084.
- [91] B. Sellergren, Molecular imprinting by noncovalent interactions Enantioselectivity and binding capacity of polymers prepared under conditions favoring the formation of template complexes, Die Makromolekulare Chemie: Macromolecular Chemistry and Physics. 190 (1989) 2703–2711. https://doi.org/10.1002/macp.1989.021901104.
- [92] D.A. Spivak, Optimization, evaluation, and characterization of molecularly imprinted polymers, Adv Drug Deliv Rev. 57 (2005) 1779–1794. https://doi.org/10.1016/j.addr.2005.07.012.
- [93] Pure Green Coffee Bean Extract Super Energizing Green Coffee Extract with 50% Chlorogenic Acid for Antioxidant Heart Health Mental Focus and Size Reduction Natural Energy Supplement for Adults., Amazon. (n.d.). https://www.amazon.com/Extract-Standardized-Chlorogenic-Supplement-Ingredients/dp/B075MPM7WM (accessed May 10, 2023).
- [94] 1115545 USP Chlorogenic acid, Sigma Aldrich. (2022). https://www.sigmaaldrich.com/US/en/product/usp/1115545.
- [95] C3878 Chlorogenic acid, Sigma Aldrich. (2022). https://www.sigmaaldrich.com/US/en/product/aldrich/c3878.

- [96] A. Burniol-Figols, K. Cenian, I. V. Skiadas, H.N. Gavala, Integration of chlorogenic acid recovery and bioethanol production from spent coffee grounds, Biochem Eng J. 116 (2016) 54–64. https://doi.org/10.1016/j.bej.2016.04.025.
- [97] D. Pujol, C. Liu, J. Gominho, M.À. Olivella, N. Fiol, I. Villaescusa, H. Pereira, The chemical composition of exhausted coffee waste, Ind Crops Prod. 50 (2013) 423–429. https://doi.org/10.1016/j.indcrop.2013.07.056.
- [98] P. Mazzafera, Chemical composition of defective coffee beans, Food Chem. 64 (1999) 547–554. https://doi.org/10.1016/S0308-8146(98)00167-8.

TOC/Abstract Graphic



Synopsis

The phenolics and flavonoids extraction is a well-studied strategy for food waste and biomass valorization, with little research on their downstream purification for commercial

applications. This study presents a methodology for their purification using molecular imprinted polymers.